

## Minimal perimeter for $N$ identical bubbles in two dimensions: calculations and simulations

S. J. COX<sup>†</sup>, F. GRANER<sup>‡</sup>||, M. FÁTIMA VAZ<sup>§</sup>, C. MONNEREAU-PITTET<sup>†</sup>  
and N. PITTET<sup>†</sup>

<sup>†</sup> Department of Physics, Trinity College, Dublin 2, Ireland

<sup>‡</sup> Unité Mixte de Recherche associée au CNRS 5588 et Université Grenoble I, Laboratoire de Spectrométrie Physique, BP 87, 38402 St Martin d'Hères Cedex, France

<sup>§</sup> Instituto de Ciência e Engenharia de Materiais e Superfícies and Departamento de Engenharia de Materiais, Instituto Superior Técnico, Avenida Rovisco Pais, 1049-001 Lisboa, Portugal

[Received 18 December 2001 and accepted in final form 12 December 2002]

### ABSTRACT

The minimal perimeter enclosing  $N$  planar regions, each being simply connected and of the same area, is an open problem, solved only for a few values of  $N$ . The problems of how to construct the configuration with the smallest possible perimeter  $E(N)$  and how to estimate the value of  $E(N)$  are considered. Defect-free configurations are classified and we start with the naïve approximation that the configuration is close to a circular portion of a honeycomb lattice. Numerical simulations and analysis that show excellent agreement to within one free parameter are presented; this significantly extends the range of values of  $N$  for which good candidates for the minimal perimeter have been found. We provide some intuitive insight into this problem in the hope that it will help the improvement in future numerical simulations and the derivation of exact results.

### §1. INTRODUCTION

What is the surface energy of a two-dimensional foam? The surface, or ‘capillary’, contribution to the energy of a two-dimensional foam is exactly its perimeter multiplied by the surface tension (Smith 1952, Weaire and Rivier 1984, Weaire and Hutzler 1999, Vaz and Fortes 2001). Can we estimate it? In other words, what is the perimeter of a finite cluster of  $N$  bubbles with *free*-boundary conditions? We intend to provide some intuitive insight into this problem and hope that it can help us to improve future numerical simulations and to derive exact results.

The total perimeter  $e$  of the cluster is the sum of the lengths of the sides. All bubbles have the same area  $A$ . We are looking for the *global* minimum in perimeter  $e$ , without constraints on the topology. This amounts to finding both the minimal perimeter  $E(N) = \min(e)$ , at fixed  $N$ , and the configuration that realizes this value (hereafter the ‘minimal’ configuration). The minimal configuration exists for all  $N$  (Morgan 2000). It has been found for  $N$  up to 2 (Morgan 2000), and a proof has

---

|| Author for correspondence. Email: graner@ujf-grenoble.fr.

recently been suggested for  $N = 3$  (Wichiramala 2002), but there are very few exact results for the value of  $E$  for  $N > 3$ , although estimates have been suggested by Vaz and Fortes (2001) for  $N$  between 1 and 22 and by Alfaro *et al.* (1990) and Morgan (1994) for  $N$  between 1 and 8. Note that more than one pattern could realize the same  $E$ .

Hales (2001) has recently proved the following ‘honeycomb conjecture’ (see also Hales (1999), Klarreich (2000) and Morgan (2000)). Consider an infinite regular honeycomb lattice of side  $L$  consisting of bubbles of identical areas  $A$  (where  $A/L^2 = 3^{3/2}/2 \approx 2.598$ ). Each side is shared by two bubbles and each bubble has six sides; so the perimeter per bubble is  $6L/2 = 3L$ . Hales has shown that this is the minimum perimeter enclosing bubbles of identical area. With periodic boundary conditions, a finite number  $N$  of bubbles with the same area  $A$  also reaches its minimal perimeter when bubbles are regular hexagons of side  $L$ : the minimal accessible perimeter is  $3NL$ . Hales’ result implies that  $E(N)/NL$  is always larger than 3 and tends towards 3 at large  $N$ , as we shall discuss.

In this paper we build on this result and estimate the minimal perimeter for a finite cluster, that is with free boundary conditions. In §2, we recall some of the constraints on possible cluster topologies and classify defect-free configurations. In §3, we present an analytical expression valid for clusters with sixfold symmetry. In §4, we present simulations for  $N = 3$  to  $N = 42$ , and then  $N = 50$  and  $N = 100$  using the Surface Evolver (Brakke 1992). In §5, we discuss the results, fit the simulations with our analytical expression and compare them with previously published estimates.

Note that throughout this paper, lower-case letters denote generic quantities:  $e$  for perimeter,  $p$  for the number of bubbles at the periphery of the cluster;  $E$  and  $P$  are the values that they reach at the minimal configuration;  $E_a$  and  $P_a$  are our analytical estimates of  $E$  and  $P$ , while  $E_s$  and  $P_s$  are the values we find in numerical simulations.

## §2. TOPOLOGICAL CLASSIFICATION

### 2.1. Total topological charge

The topological charge of a bubble in a cluster can be defined as  $q = 6 - s$ , where  $s$  is its number of sides. This quantity is additive and the total charge  $Q = \sum q$  of a cluster is  $Q = p + 6$ , where  $p$  is the number of bubbles which touch the periphery of the cluster (Smith 1952, Aste *et al.* 1996). We can thus define a similar quantity  $q^*$  (Graner *et al.* 2001): for a bubble not at the periphery,

$$q^* = 6 - s, \quad (1a)$$

and, for a bubble at the periphery,

$$q^* = 5 - s. \quad (1b)$$

Then the total of this charge is always

$$Q^* = \sum q^* = (p + 6) - p = 6, \quad (2)$$

whatever the cluster (for  $N > 1$ ).

Our purpose here is to look for candidates for the minimal configuration; we consider clusters that have an overall round shape, and topologies close to that of a honeycomb (figure 1). Typically, the clusters that we have in mind are those where the internal bubbles (those not at the periphery) have six sides; the bubbles at the

periphery have five sides, except for six bubbles that have four sides to satisfy the condition (2). In deviations from this model, defects must appear in pairs, one bubble having one more side (charge  $-1$ ) and another having one side less (charge  $+1$ ). The number  $q_-$  of negative charges in the cluster is equal to the number of defect pairs, or ‘dislocations’; the number  $q_+$  of positive charges is always equal to  $6 + q_-$ , in order to fulfil condition (2). We thus use  $q_-$  to characterize a configuration; it is the number of bubbles coloured black in figure 1. We expect that the minimal cluster will have few such defects. Charges  $\pm 2$  or more are also acceptable in principle, although we do not observe any (see below).

2.2. Candidates for the minimal configuration

As suggested above, we expect that the minimal configuration will be close to a defect-free cluster ( $q_- = 0$ ), that is a section of a hexagonal lattice with exactly six

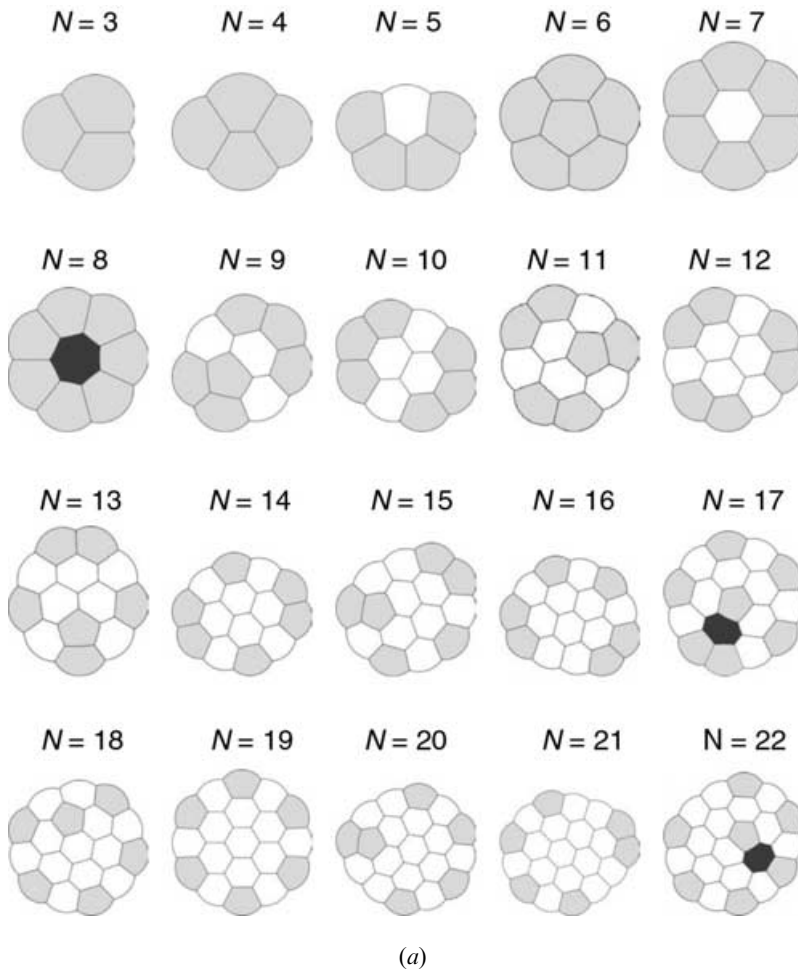
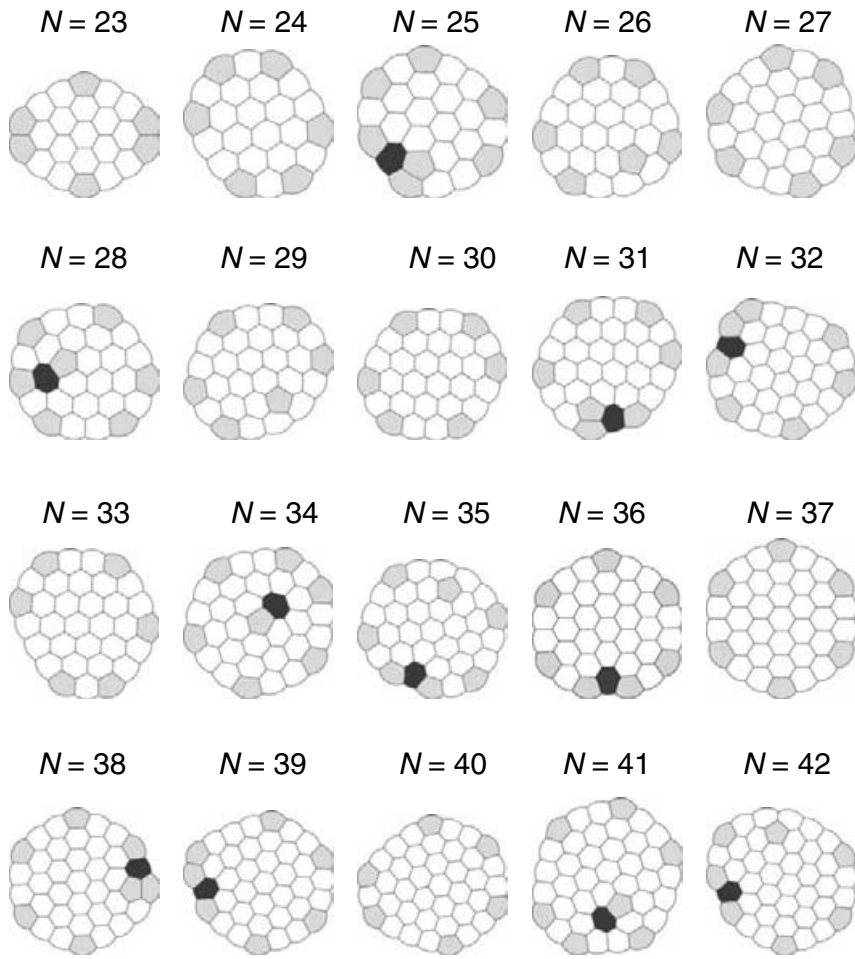
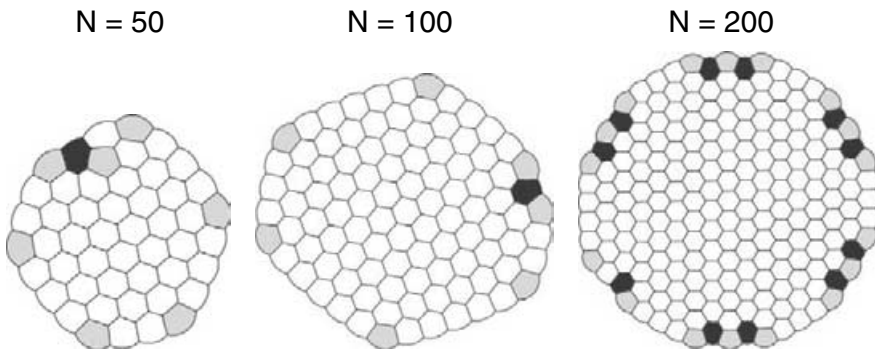


Figure 1. Candidates for the cluster configuration with the minimal perimeter found in simulations for different number  $N$  of bubbles: (a)  $N = 3$  to  $N = 22$ ; (b)  $N = 23$  to  $N = 42$ ; (c)  $N = 50$  and  $N = 100$ ; (d)  $N = 200$ . Note that we have little confidence that our suggestion for  $N = 200$  is minimal. Bubbles with a positive charge  $q^*$ , as defined in equation (1), appear in light grey; bubbles with a negative  $q^*$  appear in black.



(b)



(c)

Figure 1. (*continued*)

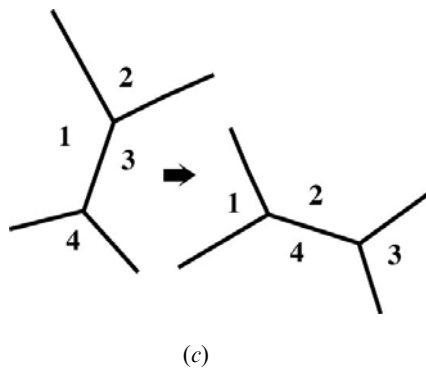
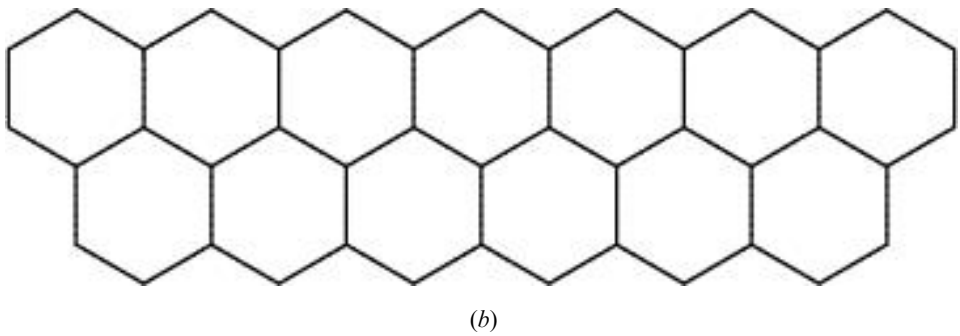
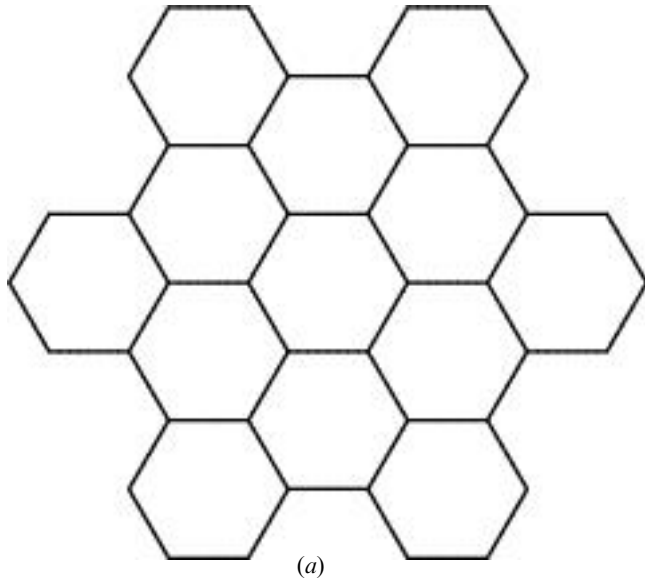


Figure 2. Explanation of the simulation procedure: (a) circular-like initial condition, for  $N = 13$ ; (b) chain-like initial condition, for  $N = 13$ ; (c) side-swapping (T1) process, in which bubbles 1 and 3 lose their common side, a new side appears between bubbles 2 and 4.

four-sided bubbles at its periphery. We can construct (K. Kassner 2001, private communication) a defect-free cluster which consists of  $i$  concentric shells (Aste *et al.* 1996), all internal cells having six sides. It is therefore sufficient to define a central  $i = 0$  shell; by definition, this kernel has no internal bubbles; it is a chain of  $n$  bubbles (analogous to the configuration shown in figure 2(b)). Varying  $n$  and  $i$  will explore a large range of defect-free clusters. The same  $N$  will appear for several pairs  $(n, i)$ . How do we choose the best pair for each  $N$ ?

If  $n > 1$ , the shell 1 has  $n + 6$  bubbles and the  $i$ th shell has  $n + 6i$  bubbles. The total number of bubbles and the number of bubbles at the periphery are thus (Vaz and Fortes 2001)

$$N(n, i) = (i + 1)(n + 3i), \quad (3a)$$

and

$$p(n, i) = 6i + n. \quad (3b)$$

respectively. The case where  $n = 1$  is special, since there are six bubbles in shell 1, and  $6i$  bubbles in the  $i$ th shell, so that

$$N(1, i) = 3i^2 + 3i + 1, \quad (4a)$$

$$p(1, i) = 6i. \quad (4b)$$

As  $n$  decreases,  $p$  also decreases, and hence the cluster looks rounder. In particular,  $n = 1$  corresponds to sixfold symmetric clusters:  $N = 1, 7, 19, \dots$

For each given value of  $N$ , there can be different pairs  $(n, i)$ . There is always at least one, namely the pair  $(N, 0)$ . It corresponds to the chain and is not a good candidate for the minimal configuration. We could look for the pair  $(n, i)$  with the lowest possible  $n$ , and hence highest  $i$ . Since this is impossible to do analytically, to our knowledge, we present an approximate approach in the next section.

### §3. ANALYTICAL EXPRESSION

#### 3.1. Cluster extracted from a honeycomb lattice

Consider an infinite honeycomb lattice and extract from it a cluster of  $N$  bubbles. In creating the cluster a number  $b$  of lattice ‘bonds’ must be broken to leave  $p$  bubbles on the periphery. They are related by (Smith 1952, Aste *et al.* 1996):

$$b = 2p + 6. \quad (5)$$

The corresponding contribution of the clusters’ external sides to the perimeter is typically of order  $bL$ . Hence twice the perimeter,  $2e$ , which was of order  $6NL$ , is now equal to  $6NL$  plus a correction of order  $bL$ . It is in fact slightly smaller, since the sides, which still meet at  $120^\circ$  angles, are no longer straight; they decrease  $e$  by relaxing to arcs of circles (Smith 1952, Weaire and Rivier 1984, Weaire and Hutzler 1999).

Estimations of a cluster’s energy based upon the number of broken bonds (Vaz and Fortes 2001) lead us to define the correction  $\varepsilon(N)$  to  $E(N)$ , of order 0.5, by the reduction in the perimeter  $E(N)/L - 3N$  associated with the presence of the cluster’s periphery:

$$E(N)/L = 3N + \varepsilon(N)[2P(N) + 6], \quad (6)$$

where we denote by  $E(N)$  and  $P(N)$  the values reached by  $e$  and  $p$  respectively in the minimal configuration. We now suggest analytical estimates of  $P(N)$  and  $E(N)$ , which we denote  $P_a$  and  $E_a$ .

3.2. Sixfold symmetric clusters

For  $N = 1, 7, 19, 37, \dots$  we presume that the sixfold symmetric configuration is actually the minimal configuration. Eliminating  $i$  in equation (4) yields

$$N > 1: P_a(N) = -3 + [3(4N - 1)]^{1/2}, \tag{7}$$

where we have excluded the unphysical case  $N = 1, P = 0$ .

Now, for simplicity we assume that the relaxation of the bubbles close to the cluster's boundary does not depend much on the number of bubbles inside the cluster. We thus assume that  $\varepsilon(N)$  does not vary much with  $N$ . Equations (6) and (7) together would thus yield

$$\frac{E_a(N)}{L} \approx 3N + 2\varepsilon[3(4N - 1)]^{1/2}. \tag{8}$$

3.3. Nearly symmetric clusters

To proceed further, we assume that for other values of  $N$  the minimal configuration is still close to a round shape. Treating  $i$  as a real parameter, we interpolate equations (7) and (8) to any value of  $N$  in equation (4); we assume that the cluster

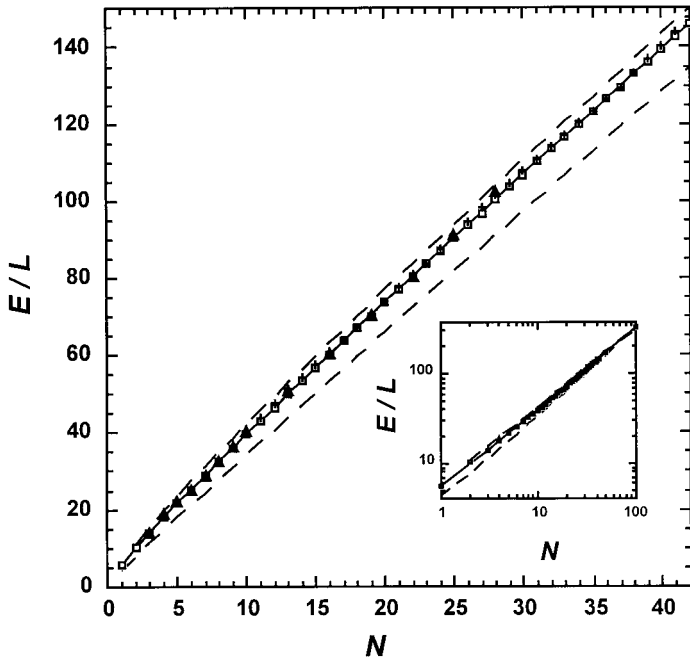


Figure 3. Estimates of the minimum perimeter  $E$  for each value of  $N$  up to 42, for  $L = 1$  ( $A = 3^{3/2}/2$ ): (—),  $E_a$ , from the analytical equation (8'); ( $\square$ ),  $E_s$ , from simulation; (+), energy of the relaxed unshuffled circular initial cluster; ( $\blacktriangle$ ), estimates from Vaz and Fortes (2001), up to  $N = 22$ , for comparison; (---), upper and lower bounds (equations (9) and (10)). The inset shows the same plot, including values  $N = 50$  and  $N = 100$ , on a log–log scale.

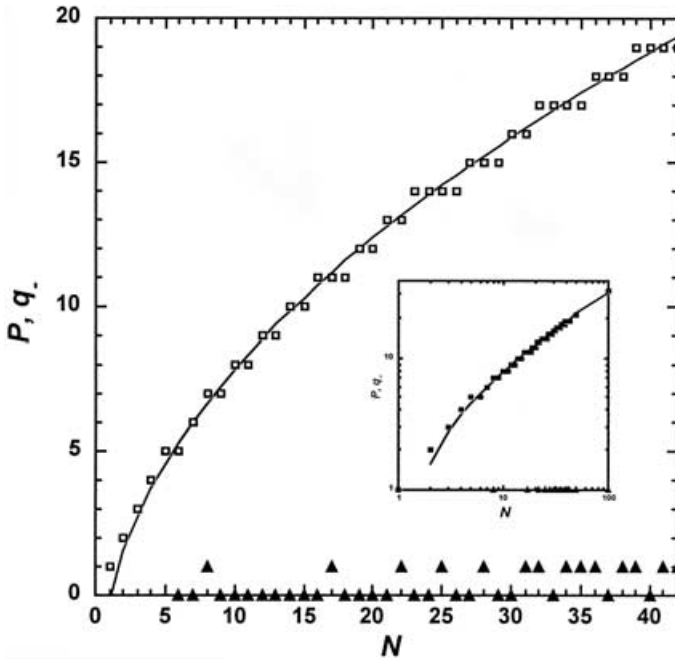


Figure 4. Number  $P_a$  of bubbles at the periphery of each cluster, from the analytical expression (7') (—)  $P_s$ , from simulations ( $\square$ ) and number  $q_-$  of topological defect pairs, from simulations ( $\blacktriangle$ ). The same plot, including the values  $N = 50$  and  $N = 100$ , on a log-log scale (hence the zero values of  $q_-$  are not shown).

chooses an integral value of  $P$  closest to the value given by the interpolated equation (7). We therefore suggest the expressions

$$P_a(N) \approx -3 + [3(4N - 1)]^{1/2}, \tag{7'}$$

$$\frac{E_a(N)}{L} \approx 3N + 2\varepsilon[3(4N - 1)]^{1/2}. \tag{8'}$$

The value of  $\varepsilon$  will be obtained by fitting equation (8') to simulations. We expect  $\varepsilon$  to be close to its value 0.447 calculated for  $N = 19$  (see table 4 of the paper by Vaz and Fortes (2001)). We thus use this value to plot equation (8') in figure 3. The value of  $P_a(N)$  is compared with simulations in figure 4.

#### § 4. SIMULATIONS

For each given value of  $N$ , the problem is to simulate a sufficient number of different topologies to have a significant chance of actually reaching the minimal configuration. Using an undirected simulation, such as a Monte-Carlo-like algorithm, would explore an unnecessary large random set of independent configurations. As mentioned, we expect and will check below that the configurations that we find are all very close to that obtained by extracting  $N$  bubbles from a honeycomb lattice. We thus choose to start from an initial configuration and locally to shuffle the cluster. This requires a careful choice of both the initial configuration and the shuffling procedure (figure 2).

#### 4.1. Initial configuration

We prepare a circular initial pattern by drawing a circle on top of a honeycomb lattice. We progressively decrease the radius of the circle, erasing all bubbles outside the circle. We make sure that the centre of the circle does not coincide with a centre of symmetry of the lattice, so that we erase the bubbles one by one. We stop when the number of remaining bubbles is exactly the prescribed number  $N$ . Most bubbles have six sides, and only a fraction of order  $N^{-1/2}$  of the bubbles are at the cluster's periphery. This method prepares an almost circular cluster (figure 2(a)), close to the minimal configuration that we find.

We also prepare an elongated initial configuration. We cut from a honeycomb lattice a long strip, two bubbles wide and  $N/2$  bubbles long. This creates a chain-like configuration, where each bubble has four neighbours except for the four bubbles at the ends (figure 2(b)). Its perimeter  $e$  is much higher than  $E(N)$ . Shuffling it also leads towards the same final configuration as with the other circular initial condition (we tried this for  $N = 12, 13$  and  $34$ ), although this is a slow procedure, both in terms of waiting for the cluster to become roughly circular and then in trying many possible 'circular' configurations to find the best.

#### 4.2. Shuffling procedure

We use the Surface Evolver (Brakke 1992) to shuffle each cluster. We perturb the cluster's perimeter gently using the Evolver's *jiggle* command; the magnitude of this random shift in the positions of each of the vertices is chosen independently for each cluster to allow for small changes in topology. We then select at each step the shortest side, and apply to it a neighbour-swapping (T1) topological process (figure

Table 1. For each  $N$  we tabulate the energy  $E_s$  of the candidate for the minimal cluster obtained from the simulations. Equation (8') allows us to estimate the value of  $\varepsilon$  for each cluster (cf. figure 5).

$N$	$E_s/L$	$\varepsilon$	$N$	$E_s/L$	$\varepsilon$
3	14.175	0.450 458	25	90.418	0.447 310
4	18.033	0.449 691	26	93.665	0.445 567
5	21.854	0.453 917	27	96.823	0.441 563
6	25.430	0.447 223	28	100.325	0.447 308
7	28.898	0.438 761	29	103.577	0.446 239
8	32.566	0.444 130	30	106.706	0.442 088
9	36.192	0.448 528	31	110.193	0.447 524
10	39.602	0.443 871	32	113.460	0.447 254
11	43.154	0.447 009	33	116.583	0.443 470
12	46.495	0.441 926	34	120.018	0.447 664
13	50.047	0.446 548	35	123.268	0.447 280
14	53.372	0.442 675	36	126.386	0.443 837
15	56.919	0.447 948	37	129.503	0.440 550
16	60.234	0.444 967	38	132.989	0.446 091
17	63.691	0.447 579	39	136.247	0.446 282
18	66.979	0.444 654	40	139.369	0.443 412
19	70.179	0.439 287	41	142.832	0.448 408
20	73.723	0.445 718	42	146.047	0.447 817
21	77.015	0.444 074	50	171.834	0.446 797
22	80.465	0.447 696	100	330.880	0.446 273
23	83.848	0.449 327	200	644.179	0.451 186
24	86.928	0.442 124			

2(c)). These T1 processes occur either close to the boundary or in the neighbourhood of defects that have migrated into the bulk of the cluster. Then we relax the configuration in quadratic mode and record its perimeter  $e$ . We iterate this shuffling-and-relaxation step, performing of the order of  $10^2$  steps for small  $N$  to  $10^4$  steps for large  $N$ , and select the configuration with the smallest perimeter  $e$ , which we record as  $E(N)$ . The resulting candidate for the minimal cluster is shown in figure 1, while the energies are listed in table 1 and plotted in figure 3. We also record its topological properties: the number  $P(N)$  of bubbles at the periphery and the number  $q_-(N)$  of topological defect pairs (both in figure 4). We have performed this procedure for each  $N$  from 3 to 42, for  $N = 50$  and for  $N = 100$ . In figure 1(d) we show the configuration obtained for  $N = 200$ . We have little confidence that this is minimal, because of the large number of negative charges; it is also unchanged from the starting configuration, suggesting that our method breaks down at large  $N$ .

## § 5. DISCUSSION

### 5.1. Agreement between analysis and simulations

Despite our rough approximations, the agreement between analytical and numerical estimates of the perimeter  $E(N)$  is surprisingly good (figure 3). We also plot analytic upper and lower bounds for the energy (F. Morgan 2002, private communication). An upper bound can be found by considering the sixfold symmetric clusters; the worst case is adding a single bubble to the boundary (e.g.  $N = 2, 8, 20, \dots$ ), for which

$$\frac{E}{L} \leq 3N + [3(4N - 5)]^{1/2} + 2. \quad (9)$$

This corresponds to  $\varepsilon \approx 0.5$ , which can be brought down to  $\varepsilon \approx 0.454$  (F. Morgan 2002, private communication). A lower bound is given by (Hales 2001, F. Morgan 2002, private communication)

$$\frac{E}{L} > 3N + [3^{3/4}(\pi/2)^{1/2} - 1.5]N^{1/2}, \quad (10)$$

which has  $\varepsilon \approx 0.196$ . We can also estimate a probable lower bound in the large- $N$  limit; when  $N$  goes to infinity, since we check that  $E/L - 3N$  goes like  $N^{1/2}$ , we first obtain that  $E/NL$  goes towards 3, as expected (Hales 2001). Equation (34) of the paper by Graner *et al.* (2001) evaluates  $\varepsilon(N)$  at large  $N$  (that is  $N \gg N^{1/2}$ , so that boundary terms are small corrections to the bulk term) by assuming that the sides of a hexagonal lattice relax into arcs of circles, so that the length  $b$  decreases by a factor  $\pi/3^{1/2}$ . This yields the estimate  $\varepsilon(N) \approx \text{const} \approx \pi/(2[3^{1/2}]) - 0.5 \approx 0.407$ . This value is probably too low, since it takes into account only the relaxation of the sides at the periphery; it neglects the change in curvature and increase in length of the sides within the bulk of the cluster, required to conserve each bubble's area.

The simulation data are also compared with the energy of the relaxed unshuffled cluster from which the simulations started. The difference between the two is always less than 3%, justifying our choice of circular starting condition; the minimal configuration is always close to a portion of a regular honeycomb. In the small- $N$  limit, Vaz and Fortes (2001) calculated  $E$  for  $N$  up to 22; their results are plotted on figure 3 and agree with the present data.

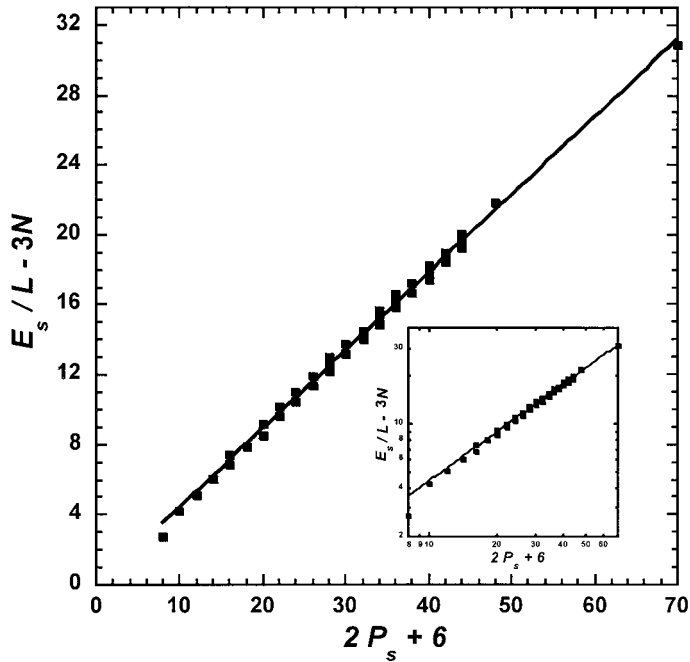


Figure 5.  $E_s - 3N$  plotted versus the number of ‘broken bonds’  $2P_s + 6$  (■), together with the linear fit with zero intercept, slope  $0.446 \pm 0.001$  (—). The inset shows the same plot, including the values  $N = 50$  and  $N = 100$ , on a log-log scale.

The number  $q_-$  of defects in our minimal clusters, shown in figure 4, is never greater than one. That is, the clusters all do well in minimizing the number of defects.

We observe that our estimates  $P_s$  and  $P_a$  of the number of bubbles at the periphery remain close to each other (figure 4); the simulated configurations are close to sixfold symmetry. As expected, the relative deviation  $(P_s - P_a)/P_a$  becomes smaller as  $N$  increases, meaning that the symmetric approximation becomes better. To estimate  $\varepsilon$  we plot  $E_s/L - 3N$  versus  $2P_s + 6$  (figure 5) and obtain a linear fit of slope 0.446, close to the value that we expected; this validates the assumption that  $\varepsilon(N)$  is constant (equation (9)). Moreover, the linear fit includes the data for  $N = 50$  and 100, increasing our confidence in these results. The values of  $\varepsilon(N)$  are given in table 1.

### 5.2. Refinements

As mentioned in §2.2, the minimal configuration requires a compromise between two conditions.

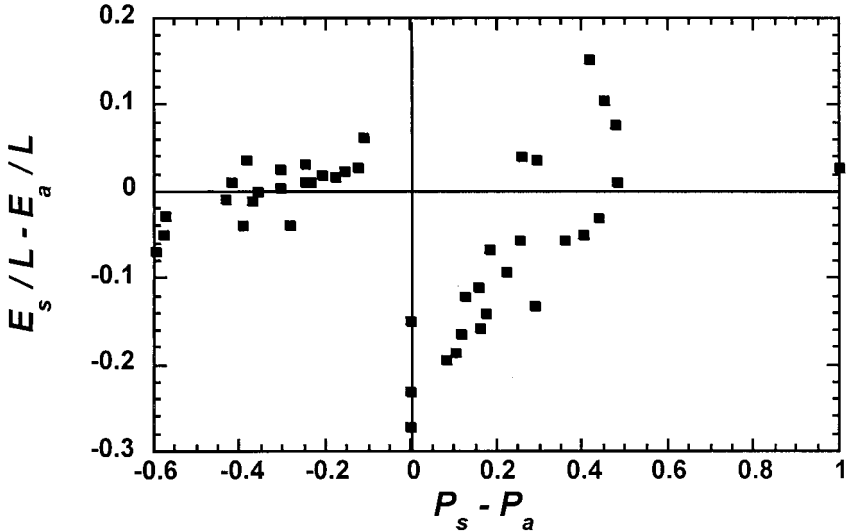
- (i) The periphery of the cluster should be as round as possible.
- (ii) While defects are unavoidable, their total number should be as low as possible.

This optimization is subject to two trivial but strong constraints.

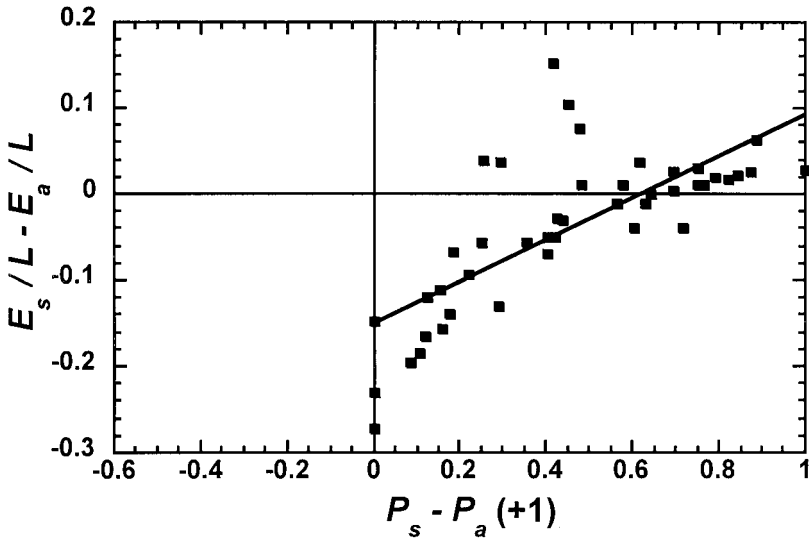
- (iii) The number of bubbles is an integer number.
- (iv) The topology is one that is actually realizable.

The analytical expressions (equations (7') and (8')) are only an optimization of conditions (i) and (ii). On the other hand, the simulations do take into account conditions (iii) and (iv). It is thus interesting to focus on their differences.

We observe that the deviation  $P_s - P_a$  from sixfold symmetry correlates with the presence of a defect (variable  $q_-$  in figure 4). At first, we thus expected it would also correlate with the error  $E_s - E_a$  of our analytical approximation. However, in figure 6(a), data separate into two groups. It seems that the perimeter of a cluster is related



(a)



(b)

Figure 6. (a) Error  $E_s - E_a$  of our analytical approximation versus the deviation  $P_s - P_a$  from symmetry. (b) The same plot, with  $P_s - P_a + 1$  replacing  $P_s - P_a$  each time that it is negative (see text): (—) (linear fit of slope 0.25), guide for the eye.

to the ‘fractional part’ of  $P_s - P_a$ , that is its distance to the integer immediately below. This appears in figure 6(b) where, each time that  $P_s - P_a$  was negative, we have replaced it by  $P_s - P_a + 1$ ; we now observe a correlation with the error  $E_s - E_a$ .

In addition to condition (ii), Graner *et al.* (2001) also derived a formal analogy between the energy of defects and the interaction energy of electrostatic charges. Accordingly, the perimeter should be lower when charges of the same sign are as far as possible from each other, and charges of different sign are close to each other. This is difficult to quantify and test, especially owing to topological constraints (the above conditions (iii) and (iv)). However, we note that figure 1 conveys exactly this impression.

Note that the sixfold symmetry is striking for all  $N$  up to 100 (figure 1), but for  $N = 200$  its effect is not felt any longer. This might be the limit of validity of our assumption (equation (7)); it should probably be replaced, at higher  $N$ , by an assumption of circular symmetry. We are currently trying to refine both the analysis and the simulations using a more efficient simulated annealing procedure. We also apply this approach to polydisperse clusters, that is clusters with bubbles of different areas (Vaz *et al.* 2002).

## §6. CONCLUSIONS

In this paper, we have examined the minimum perimeter enclosing a cluster of  $N$  planar, simply connected bubbles of identical area  $A = 3^{3/2}L^2/2 \approx 2.598L^2$ . We considered the problem of how to construct the configuration with the smallest possible perimeter  $E(N)$ , and how to estimate the value of  $E(N)$ . We started with a configuration that is close to a circular portion of a honeycomb lattice and wrote a simple analytical expression for the perimeter (equation (8')) that showed excellent agreement with our simulations for  $N$  up to 42, for  $N = 50$  and for  $N = 100$ . A catalogue of candidates for the minimal cluster has been given; these clusters show no more than a single defect, and the number of bubbles on the periphery agrees closely with equation (7'). We hope that, with a similar approach and an improved simulation method, it should soon be possible to provide minimal candidates for larger  $N$ , although a rigorous proof that these are the true minimizers remains a much more difficult problem.

## ACKNOWLEDGEMENTS

We wish to thank Klaus Kassner for his suggestion concerning cluster classification, Manuel Fortes and Renaud Delannay for critically reading the manuscript, Frank Morgan for his patient explanation of energy bounds and Marie-Line Chabanol, Marc Hindry, and Denis Weaire for interesting discussions. F.G. thanks Trinity College, Dublin, and Instituto Superior Técnico, and F.V. thanks Trinity College, Dublin and Laboratoire de Spectrométrie Physique, for their hospitality. N.P. was supported by Enterprise Ireland, C.M.-P. and S.J.C. were supported by Marie Curie fellowships, and F.G. benefited from the ULYSSES France–Ireland exchange programme.

## REFERENCES

- ALFARO, M., BROCK, J., FOISY, J., HODGES, N., ZIMBA, J., and MORGAN, F., 1990, Report, Geometry Group of the Williams College SMALL Undergraduate Research Project.  
 ASTE, T., BOOSÉ, D., and RIVIER, N., 1996, *Phys. Rev. E*, **53**, 6181.  
 BRAKKE, K., 1992, *Exp. Math.*, **1**, 141.

- GRANER, F., JIANG, Y., JANIAUD, E., and FLAMENT, C., 2001, *Phys. Rev. E*, **63**, 11 402.
- HALES, T. C., 1999, *Sci. News, Washington DC*, **156**, 60; 2001, *Discrete Comput. Geom.*, **25**, 1.
- KLARREICH, E., 2000, *Am. Sci.*, **88**, 152.
- MORGAN, F., 1994, *Am. Math. Mon.*, **101**, 343; 2000, *Geometric Measure Theory: A Beginner's Guide*, third edition (Boston, Massachusetts: Academic Press).
- SMITH, C. S., 1952, *Metal Interfaces* (Cleveland, Ohio: American Society for Metals), p. 65.
- VAZ, M. F., and FORTES, M.A., 2001, *J. Phys.: condens. Matter*, **13**, 1395.
- VAZ, M. F., GRANER, F., and FORTES, M. A., 2002, *Phil. Mag. Lett.*, **82**, 575.
- WEAIRE, D., and HUTZLER, S., 1999, *The Physics of Foams* (Oxford: Clarendon).
- WEAIRE, D., and RIVIER, N., 1984, *Contemp. Phys.*, **25**, 59.
- WICHIRAMALA, W., 2002, PhD Thesis, University of Illinois.